

The mass distribution of coarse particulate organic matter

J. M. Turowski et al.

The mass distribution of coarse particulate organic matter exported from an alpine headwater stream

J. M. Turowski^{1,2}, A. Badoux¹, K. Bunte³, C. Rickli¹, N. Federspiel^{1,4}, and M. Jochner^{1,5}

¹Swiss Federal Research Institute WSL, Zürcherstrasse 111, 8903 Birmensdorf, Switzerland

²Helmholtz Centre Potsdam, GFZ German Research Centre for Geosciences, Telegrafenberg 14473 Potsdam, Germany

³Engineering Research Center, Colorado State University, Fort Collins, CO 80523, USA

⁴CSD Engineers SA, Hessesstrasse 27d, 3097 Liebefeld (Berne), Switzerland

⁵Institute of Geography of the University of Berne (GIUB), Hallerstrasse 12, 3012 Berne, Switzerland

Received: 19 April 2013 – Accepted: 29 April 2013 – Published: 15 May 2013

Correspondence to: J. M. Turowski (turowski@gfz-potsdam.de)

Published by Copernicus Publications on behalf of the European Geosciences Union.

Title Page

Abstract

Introduction

Conclusions

References

Tables

Figures

⏪

⏩

◀

▶

Back

Close

Full Screen / Esc

Printer-friendly Version

Interactive Discussion

Abstract

Coarse particulate organic matter (CPOM) particles span sizes from 1 mm, with masses less than 1 mg, to large logs and whole trees, which may have masses of several hundred kilograms. Different size and mass classes play different roles in stream environments, from being the prime source of energy in stream ecosystems to macroscopically determining channel morphology and local hydraulics. We show that a single scaling exponent can describe the mass distribution of CPOM transported in the Erlenbach, a steep mountain stream in the Swiss Prealps. This exponent takes an average value of -1.8 , is independent of discharge and valid for particle masses spanning almost seven orders of magnitude. Together with a rating curve of CPOM transport rates with discharge, we discuss the importance of the scaling exponent for measuring strategies and natural hazard mitigation. Similar to CPOM, the mass distribution of in-stream large woody debris can likewise be described by power law scaling distributions, with exponents varying between -1.8 and -2.0 , if all in-stream material is considered, and between -1.4 and -1.8 for material locked in log jams. We expect that scaling exponents are determined by stream type, vegetation, climate, substrate properties, and the connectivity between channels and hillslopes. However, none of the descriptor variables tested here, including drainage area, channel bed slope and forested area, show a strong control on exponent value. The number of streams studied in this paper is too small to make final conclusions.

1 Introduction

Coarse particulate organic matter (CPOM) plays multiple roles in stream systems. Defined as pieces of organic matter with a diameter larger than 1 mm, it spans the range from leave and wood fragments over twigs and branches to logs and complete trees. Large woody debris (LWD), at the top of this range, is often defined as having a minimum diameter of 0.1 m and a minimum length of 1 m (e.g., Wohl and Jaeger, 2009),

ESurfD

1, 1–29, 2013

The mass distribution of coarse particulate organic matter

J. M. Turowski et al.

Title Page

Abstract

Introduction

Conclusions

References

Tables

Figures

⏪

⏩

◀

▶

Back

Close

Full Screen / Esc

Printer-friendly Version

Interactive Discussion



rates and dry masses of CPOM pieces heavier than 0.1 g moving in the Erlenbach, a headwater stream in the Swiss Prealps, using several sampling methods over a large range of discharges. In addition, we collected data on in-stream LWD size distributions for the Erlenbach, and compared it to data from ten other mountain streams in Switzerland (Rickli and Bucher, 2006), and from the literature. We discuss the use of scaling relations in data analysis and natural hazard mitigation.

2 Field site

The Erlenbach is a small headwater stream located near Einsiedeln in the Swiss Prealps (Fig. 1), where scientific observations have been conducted since the late 1960s (Hegg et al., 2006). The channel bed has a mean gradient of around 18 % and drains an area of 0.7 km² at the main observation site. About 40 % of the total catchment area is forested, with the remaining 60 % consisting of wetland and alpine meadows. The forest dominantly comprises Norway Spruce (*Picea abies*) and European Silver Fir (*Abies alba*), intermingled with some Alder (*Alnus spec.*), and a wide variety of shrubs and ground plants (Schleppi et al., 1999). The Erlenbach is a step-pool channel with high sediment load, which is mainly supplied by a series of slow-moving landslides along the channel banks (Schuerch et al., 2006; Turowski et al., 2009; Molnar et al., 2010). There are two discharge gauges located immediately upstream and downstream of a sediment retention basin where automatic basket samplers and indirect bedload sensors for sediment transport measurements are available (Rickenmann et al., 2012; Turowski et al., 2011). Discharge is continuously recorded at 10 min intervals, and at 1 min intervals during bedload transport events. Unless otherwise stated, we used the 10 min data of the upper gauge throughout this paper. The mean discharge at the Erlenbach is 39 l s⁻¹, and during dry weather it is typically below 10 l s⁻¹. Floods, driven mainly by convective summer storms, are common, and stream flow quickly responds to heavy rainfall. The yearly return discharge is approximately 2000 l s⁻¹. The highest discharge

The mass distribution of coarse particulate organic matter

J. M. Turowski et al.

Title Page

Abstract

Introduction

Conclusions

References

Tables

Figures

⏪

⏩

◀

▶

Back

Close

Full Screen / Esc

Printer-friendly Version

Interactive Discussion



The mass distribution of coarse particulate organic matter

J. M. Turowski et al.

Title Page

Abstract

Introduction

Conclusions

References

Tables

Figures

⏪

⏩

◀

▶

Back

Close

Full Screen / Esc

Printer-friendly Version

Interactive Discussion



The automatic basket samplers consist of metal cubes with 1 m edges (Rickenmann et al., 2012). The baskets' walls and floors are made of a metal mesh of square holes with an edge length of 10 mm. Sampling is triggered when thresholds of stage level and indirect bedload sensor activity are exceeded. The entire flow width is sampled at discharges up to around 1500 l s^{-1} . Samples were taken between 2009 and 2012 during rainfall-driven floods.

Organic matter from basket and trap samples was separated from clastic material and weighed wet in the field. Subsequently, the samples were oven-dried over 24 h at 80°C in the laboratory, and the dry mass was obtained. For a total of 18 out of 42 basket samples, all pieces of organic matter heavier than about 1 g were individually weighed and measured. In samples taken at lower discharges with the bedload samplers, all pieces heavier than 0.1 g or 0.01 g were individually weighed, depending on the total number of pieces.

After two large floods in July 1995 and August 2010 with peak discharges of $\sim 10\,100 \text{ l s}^{-1}$ and $\sim 9300 \text{ l s}^{-1}$, respectively (10 min data) (Turowski et al., 2009, 2013), pieces of woody debris with diameters larger than 0.05 m were collected from the sediment retention basin, and their lengths and diameters were measured in the field. The measurements were converted to mass assuming a cylindrical shape and a dry wood density of 410 kg m^{-3} , which is typical for the Norway Spruce (*Picea Abies*) that is common in the catchment. To obtain a representative discharge for these data points, we assumed that large pieces of wood are dominantly transported at discharges higher than 5000 l s^{-1} , using discharge measurements at 1 min resolution. This discharge was exceeded for 20 and 18 min, respectively, during the events, and accordingly we averaged all discharge measurements exceeding it.

In addition to sampling material transported by the stream, the length and diameter of all woody debris pieces stored in log jams longer than 1 m (LWD) were recorded in the field. LWD masses were calculated assuming a cylindrical shape and a dry wood density of 410 kg m^{-3} .

4 Results and analysis

The occurrence of sampled CPOM particles is tightly related to their masses; the number of CPOM pieces in transport strongly decreased with increasing particle mass. At particle masses greater than a threshold value of ~ 1 g for the basket samples and ~ 3 kg for the retention basin samples, the relative frequencies of occurrence of masses in the samples plot on a straight line in log-log space (Fig. 2). No such threshold was observed for the bedload trap data, because the smaller net size trapped finer particles. The relationships can be described by the equation:

$$C = kM^{-\alpha}. \quad (1)$$

Here, C is the relative fraction of CPOM of the respective particle mass M , k is a constant and α is the scaling exponent. The relative fraction is proportional to the measured fraction of CPOM in each mass class, but may be normalized for example by bin width. For each CPOM sample, scaling exponents were obtained by fitting a linear relation to the log-transformed data in the long falling branch. Minimum and maximum values of α were 1.41 and 2.26, respectively, and the mean was 1.84 ± 0.04 (range gives standard error of the mean). For all discharges where samples contained enough individual pieces of material to derive a relation between piece numbers and mass, scaling exponents were independent of discharge (Fig. 3).

By dividing total CPOM mass by sampling time, we obtained CPOM transport rates. These show a clear relation with discharge, defined by a straight line in log-log space (Fig. 4). However, it needs to be born in mind that we used different sampling devices with different net sizes (bedload traps: 6 mm; basket samplers: 10 mm; LWD from the retention basin). Below we will show how the scaling relation of Eq. (1) can be used to make the samples comparable.

The mass distribution of coarse particulate organic matter

J. M. Turowski et al.

Title Page

Abstract

Introduction

Conclusions

References

Tables

Figures

⏪

⏩

◀

▶

Back

Close

Full Screen / Esc

Printer-friendly Version

Interactive Discussion



As long as the scaling exponent $\alpha > 1$, the total mass M_{tot} of the sample above a minimum mass M_{min} can be obtained by using the integral

$$M_{\text{tot}} = \int_{M_{\text{min}}}^{\infty} kM^{-\alpha} dM = \frac{kM_{\text{min}}^{1-\alpha}}{\alpha - 1}. \quad (2)$$

The ratio between the total mass $M_{1,\text{tot}}$ larger than a threshold mass $M_{1,\text{min}}$, and the total mass $M_{2,\text{tot}}$ larger than a threshold mass $M_{2,\text{min}}$ can thus be written as:

$$\frac{M_{1,\text{tot}}}{M_{2,\text{tot}}} = \left(\frac{M_{1,\text{min}}}{M_{2,\text{min}}} \right)^{1-\alpha}. \quad (3)$$

To be able to compare the samples taken with bedload traps and basket samplers, we estimated the minimal particle mass that is sampled representatively by the baskets at 1 g. The lack of a further increase in relative counts for smaller particles indicates that not all material of smaller masses was sampled (see Fig. 2). Particles lighter than 1 g were omitted from the samples, and the remainder was used for further analysis. For basket samples where the mass distribution was not measured, we used the average fraction of mass contributed by 1 g particles to the total mass from the basket samples where it was measured. This value of 0.48 was multiplied with the total measured CPOM mass. For each basket sample, the total mass above 0.1 g was then calculated using Eq. (3). For the bedload trap samples, we only used samples for which the mass distribution was measured and which included individual pieces heavier than 0.1 g.

The corrected samples were plotted against discharge to obtain a rating curve (Fig. 4). The rating exponent of 4.47 was obtained by fitting a linear relationship to the log-transformed data. The data points from the two extreme events were not included in the fit. There, all particles heavier than about 3 kg (dry mass) were sampled representatively, and the measured mass of 219 kg was extrapolated down to piece masses of 0.1 g using the average scaling exponent of 1.84 (Fig. 3). The resulting points plot

The mass distribution of coarse particulate organic matter

J. M. Turowski et al.

Title Page

Abstract

Introduction

Conclusions

References

Tables

Figures

⏪

⏩

◀

▶

Back

Close

Full Screen / Esc

Printer-friendly Version

Interactive Discussion



close to the rating curve between CPOM transport rate and discharge derived from the trap and basket measurements and confirm the validity of the CPOM transport rating relation at high discharges (Fig. 4).

Locked in nine log jams along the Erlenbach channel, we measured a total of 79 pieces of LWD. The size distribution of this material likewise decreased with particle mass (Fig. 5), although with a value of 1.26 the scaling exponent was lower than observed for transported material. Scaling exponents similar to those from the Erlenbach were also obtained from 6700 wood pieces measured in ten other Swiss mountain streams (Rickli and Bucher, 2006; see Table 1). Power function scaling exponents ranged within 1.78 to 2.04 for all wood pieces in the channel and within 1.39 and 1.75 for those locked in log jams (Fig. 6) (the two extraordinary low values were from derived from small sample sizes at the Brueggwaldbach and the Grossbach are unreliable). Scaling exponents appeared unrelated to basin area size, stream width and gradient, and the percent forested area (Fig. 7).

5 Discussion

5.1 Masses of CPOM input and piece break down

Various processes in the stream work together to produce the observed mass distribution of CPOM particles from the original mass distribution of organic material supplied to the stream. Coarse particulate organic matter enters the stream either as litter fall directly from the trees or blown in by wind, or via the stream banks either as material advected into the channel by landslides and snow creep, or flushed into it by overland flow. Litter typically comprises leaves with dry masses below 0.1 g and twigs with masses smaller than about 5 g. Larger material, often whole trees, can enter the channel due to wind throw or by riding on top of landslides. A number of slow-moving landslide complexes have been identified along the banks of the Erlenbach, causing efficient channel-hillslope connectivity (Schuerch et al., 2006). Trees, tree trunks and large

The mass distribution of coarse particulate organic matter

J. M. Turowski et al.

Title Page

Abstract

Introduction

Conclusions

References

Tables

Figures

⏪

⏩

◀

▶

Back

Close

Full Screen / Esc

Printer-friendly Version

Interactive Discussion



The mass distribution of coarse particulate organic matter

J. M. Turowski et al.

Title Page

Abstract

Introduction

Conclusions

References

Tables

Figures

⏪

⏩

◀

▶

Back

Close

Full Screen / Esc

Printer-friendly Version

Interactive Discussion



branches are abundant in the Erlenbach channel and along the banks. Thus, based on preliminary data from litter traps installed above the stream channel and from field observations, we can assume that the input distribution of CPOM masses is strongly bimodal, with one peak lying between 0.1 g and 1 g (leaves and twigs), and one at > 100 kg (whole trees). The mass distribution of the material flushed out of the stream therefore does not correspond to the input distribution, and in-stream processes must break down larger material while it resides in the channel. These processes can be broadly divided into physical, chemical and biological processes (although these may interact) (Harmon et al., 1986; Merten et al., 2013; Webster et al., 1999). The physical processes include breakage and detachment of pieces by fluid stressing, grinding of woody debris by gravel bedload, wood-wood interaction (for example a floating log impacting stationary material), or the break-up of log jams (Harmon et al., 1986). In addition, wetting/drying cycles and possibly freezing/thawing may lead to swelling and cracking of wood. Parts of woody material can be dissolved in water and carried out in solution (e.g., Yoshimura et al., 2010). This loss of material may destabilize the structure of the debris and make it more prone to physical erosion. Finally, bacteria and fungi colonize dead wood and decompose it, while animals, for example fresh-water invertebrates or certain types of insects such as Plecoptera larvae, may attack CPOM pieces to obtain food or to create shelter (e.g., Webster and Benfield, 1986; Montemarano et al., 2007). As pointed out by Hassan et al. (2005), little is known about the relative importance of different wood depletion processes. Merten et al. (2013) found that physical breakage was responsible for a mass loss of around 7.3% in LWD, while decay contributed around 1.9% in streams in northern Minnesota, USA. However, it is currently unclear how these results transfer to other regions. In addition, it is not known what piece sizes are produced by the various decay processes, how fluvial transport affects the CPOM/LWD size distribution, and how exactly the different processes play together to produce the observed output mass distribution.

5.2 Implications for sampling strategies

Using the rating curve and measured discharge, CPOM export during individual events and over longer time scales can be calculated. Due to the strong dependence of CPOM on discharge with a rating curve exponent of 4.47, CPOM transport is dominated by large discharge events. For instance, applying the rating curve to the measured discharge from the extreme event in August 2010, this event alone exported nearly 2×10^6 kg of CPOM, comprising 94 % of the total export for the year 2010. Without deriving a detailed rating curve, similarly strong dependences on discharge have been reported previously (e.g., Fisher and Likens, 1973). This suggests that CPOM measurements conducted at low discharges give an incomplete picture of overall CPOM transport. However, if the scaling exponent of the mass distribution is known, and for a given event a certain size fraction has been sampled representatively, the complete CPOM export can be calculated. Our study results suggest that CPOM export for all size fractions can be estimated from is the volumes of LWD exported in a large event, for example by measuring piece sizes trapped in a reservoir or by video monitoring the passage of wood pieces (e.g., MacVicar and Piégay, 2012; MacVicar et al., 2009; Seo et al., 2008; West et al., 2011). In addition to scaling down from LWD deposits to estimate CPOM export, the scaling functions also permit scaling up from CPOM transport to estimate LWD transport. The combination of a rating curve of CPOM transport rates with discharge and the mass distribution obtained from samples collected at low and intermediate flows can be used to discuss the mobility of LWD.

5.3 Mobility of large woody debris and hazard assessment

Floating wood is a source of hazard in many mountain streams (e.g., Mazzorana et al., 2011; Rickenmann, 1997). For example, woody debris can jam in channel constrictions or at bridges, which may trap sediment and force water to overflow and leave the channel. In addition, logs floating at the surface of the stream can achieve considerable velocities, leading them to cause considerable damage upon impact on infrastructure

The mass distribution of coarse particulate organic matter

J. M. Turowski et al.

Title Page

Abstract

Introduction

Conclusions

References

Tables

Figures

⏪

⏩

◀

▶

Back

Close

Full Screen / Esc

Printer-friendly Version

Interactive Discussion



in log jams, and is moved less frequently than smaller material. This reflects the selective transport of large pieces of wood and the fact that jamming makes coarse material less mobile. The scaling exponents do not show a strong correlation with any of the tested predictor variables mean elevation above sea level, drainage area, channel bed slope, channel width, forested area, and percent forested area (Fig. 7). However, the range of conditions in the investigated streams is small and a final assessment would need a larger data base.

Not many reports of size distributions of CPOM can be found in the literature, and the majority of the available studies used piece diameter as descriptor variable (e.g., Harmon et al., 1986; Jackson and Sturm, 2002). We were able to find a single study using volume as a descriptor variable (Hogan, 1987). We digitized the data for the unlogged reaches, and found power law scaling with exponent values of 1.72 for the small watershed (3.9 km²), 1.61 for the medium watershed (6.9 km²) and 1.90 for the large watershed (20.2 km²) (here, the depiction of “small”, “medium” and “large” is after Hogan’s (1987) own terminology). MacVicar and Piégay (2012) reported the distribution of LWD piece length in transport, observed using a video camera during floods of the Ain River, France. We digitized that data and converted from piece length to mass using a power-law fitted to the relationship of Erlenbach LWD taken from the retention basin samples (Fig. 8). Clearly, this is a rough approach, but when the data of MacVicar and Piégay (2012) are converted to mass using this relationship, a well-defined power-law scaling with a scaling exponent of 1.62 is obtained (Fig. 9). The scaling exponent is similar to the one observed at the Erlenbach (1.84). The slightly smaller value implies the occurrence of large CPOM pieces is more frequent in comparison. The Ain River is a much larger stream than the Erlenbach, with a drainage area of 3630 km² (compared to 0.7 km² at the Erlenbach) and a width of ~65 m (compared to ~4 m at the Erlenbach). LWD pieces longer than the channel width are rarely transported (Bilby and Ward, 1989; Nakamura and Swanson, 1993), and it has been shown in field studies that LWD moves further and more frequently in larger streams (e.g., Lienkamper and Swanson, 1987). Thus, the slightly greater abundance of long pieces in the Ain River

The mass distribution of coarse particulate organic matter

J. M. Turowski et al.

Title Page

Abstract

Introduction

Conclusions

References

Tables

Figures

⏪

⏩

◀

▶

Back

Close

Full Screen / Esc

Printer-friendly Version

Interactive Discussion



The mass distribution of coarse particulate organic matter

J. M. Turowski et al.

Title Page

Abstract

Introduction

Conclusions

References

Tables

Figures

◀

▶

◀

▶

Back

Close

Full Screen / Esc

Printer-friendly Version

Interactive Discussion



Rickli, C. and Bucher, H.: Einfluss ufernaher Bestockung auf das Schwemmholtzvorkommen in Wildbächen, technical report, Swiss Federal Research Institute WSL, 94 pp., www.wsl.ch/fe/gebirgshydrologie/wildbaeche/projekte/schwemmholtzvorkommen/rickli-shber_261007.pdf, 2006.

5 Schleppi, P., Muller, N., Edwards, P. J., und Bucher, J. B.: Three years of increased nitrogen deposition do not affect the vegetation of a montane forest ecosystem, *Phyton*, 39, 197–204, 1999.

Schuerch, P., Densmore, A. L., McArdeell, B. W., and Molnar, P.: The influence of landsliding on sediment supply and channel change in a steep mountain catchment, *Geomorphology*, 78, 222–235, doi:10.1016/j.geomorph.2006.01.025, 2006.

10 Seo, J. I., Nakamura, F., Nakano, D., Ichiyangi, H., and Chun, K. W.: Factors controlling the fluvial export of large woody debris, and its contribution to organic carbon at watershed scales, *Water Resour. Res.*, 44, W04428, doi:10.1029/2007WR006453, 2008.

15 Turowski, J. M., Yager, E. M., Badoux, A., Rickenmann, D., and Molnar, P.: The impact of exceptional events on erosion, bedload transport and channel stability in a step-pool channel, *Earth Surf. Proc. Land.*, 34, 1661–1673, doi:10.1002/esp.1855, 2009.

Turowski, J. M., Badoux, A., and Rickenmann, D.: Start and end of bedload transport in gravel-bed streams, *Geophys. Res. Lett.*, 38, L04401, doi:10.1029/2010GL046558, 2011.

20 Turowski, J. M., Badoux, A., Leuzinger, J., and Hegglin, R.: Large floods, alluvial overprint and bedrock erosion, *Earth Surf. Proc. Land.*, doi:10.1002/esp.3341, in press, 2013.

Webster, J. R. and Benfield, E. F.: Vascular plant breakdown in freshwater ecosystems, *Annu. Rev. Ecol. Evol. Syst.*, 17, 567–594, 1986.

Webster, J. R. and Meyer, J. L.: Organic matter budgets for streams: A synthesis, *J. N. Am. Benthol. Soc.*, 16, 141–161, 1997.

25 Webster, J. R., Benfield, E. F., Ehrman, T. P., Schaeffer, M. A., Tank, J. L., Hutchens, J. J., and D'Angelo, D. J.: What happens to allochthonous material that falls into streams? A synthesis of new and published information from Coweeta, *Freshwater Biol.*, 41, 687–705, 1999.

West, A. J., Lin, C.-W., Lin, T.-C., Hilton, R. G., Liu, S.-H., Chang, C.-T., Lin, K.-C., Galy, A., Sparkes, R. B., and Hovius, N.: Mobilization and transport of coarse woody debris to the oceans triggered by an extreme tropical storm, *Limnol. Oceanogr.*, 56, 77–85, doi:10.4319/lo.2011.56.1.0077, 2011.

30 Wohl, E. and Jaeger, K.: A conceptual model for the longitudinal distribution of wood in mountain streams, *Earth Surf. Proc. Land.*, 34, 329–344, doi:10.1002/esp.1722, 2009.

Yoshimura, C., Fujii, M., Omura, T., and Tockner, K.: Instream release of dissolved organic matter from coarse and fine particulate organic matter of different origins, *Biochemistry*, 100, 151–165, doi:10.1007/s10533-010-9412-y, 2010.

ESurfD

1, 1–29, 2013

The mass distribution of coarse particulate organic matter

J. M. Turowski et al.

Title Page

Abstract

Introduction

Conclusions

References

Tables

Figures



Back

Close

Full Screen / Esc

Printer-friendly Version

Interactive Discussion



The mass distribution of coarse particulate organic matter

J. M. Turowski et al.

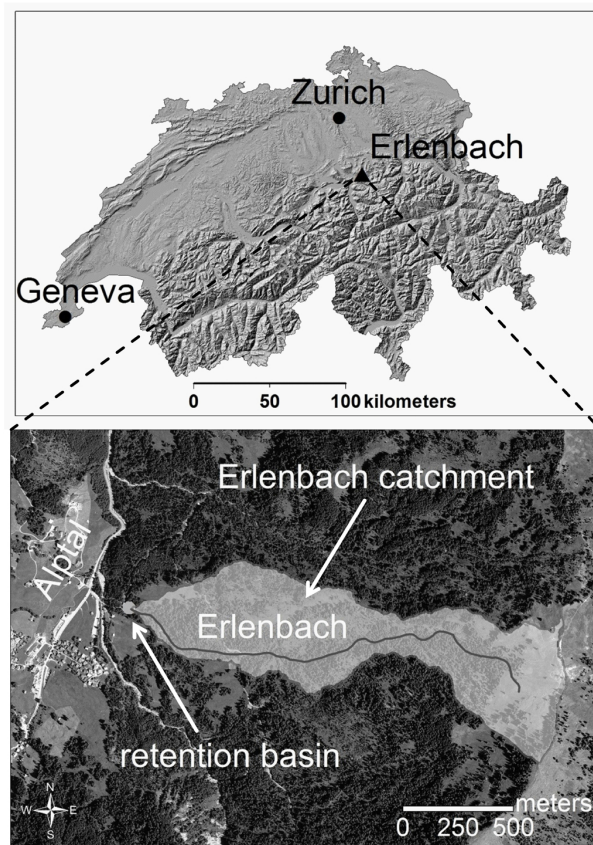


Fig. 1. Location map of the Erlenbach in Switzerland and bird's eye view of the catchment.

[Title Page](#)[Abstract](#)[Introduction](#)[Conclusions](#)[References](#)[Tables](#)[Figures](#)[◀](#)[▶](#)[◀](#)[▶](#)[Back](#)[Close](#)[Full Screen / Esc](#)[Printer-friendly Version](#)[Interactive Discussion](#)

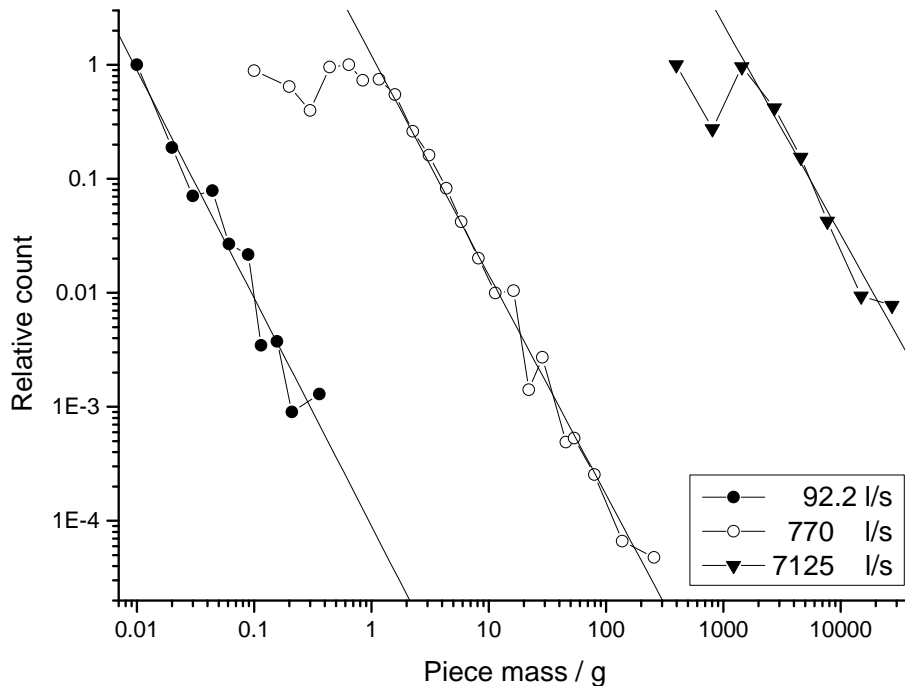


Fig. 2. Examples of histograms of CPOM particle masses at three different discharges, spanning two orders of magnitude in discharge and more than six orders of magnitude in particle mass. To reduce the extent of the axes, and to demonstrate the general similarity of the CPOM piece count vs. mass relations, each of the histograms was normalized such that the most common fraction plots at a relative count of one. The sample collected at 92.2 l/s is typical of those taken with bedload traps, the one at 770 l/s of those with basket samplers, and the one at 7125 l/s was collected from the debris basin.

The mass distribution of coarse particulate organic matter

J. M. Turowski et al.

Title Page

Abstract Introduction

Conclusions References

Tables Figures

⏪ ⏩

⏴ ⏵

Back Close

Full Screen / Esc

Printer-friendly Version

Interactive Discussion



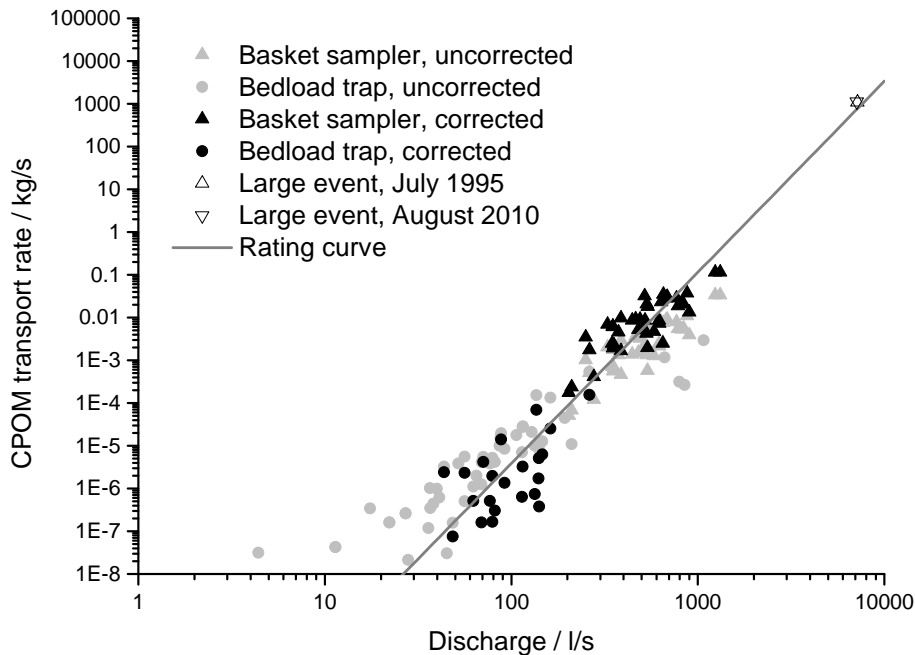


Fig. 4. CPOM transport rates as a functions of discharge. Both the untreated data (light grey) and the values corrected for transport rates of all particles heavier than 0.1 g (black) are shown. The rating curve is of the form $Q_{\text{CPOM}} = aQ^b$, with $a = 4.42 \times 10^{-15}$ and $b = 4.47 \pm 0.21$, with an R value of 0.94. The two data points from the large events (open triangles) plot nearly at the same location. They were not used in the regression to obtain the rating curve.

The mass distribution of coarse particulate organic matter

J. M. Turowski et al.

Title Page	
Abstract	Introduction
Conclusions	References
Tables	Figures
⏪	⏩
◀	▶
Back	Close
Full Screen / Esc	
Printer-friendly Version	
Interactive Discussion	



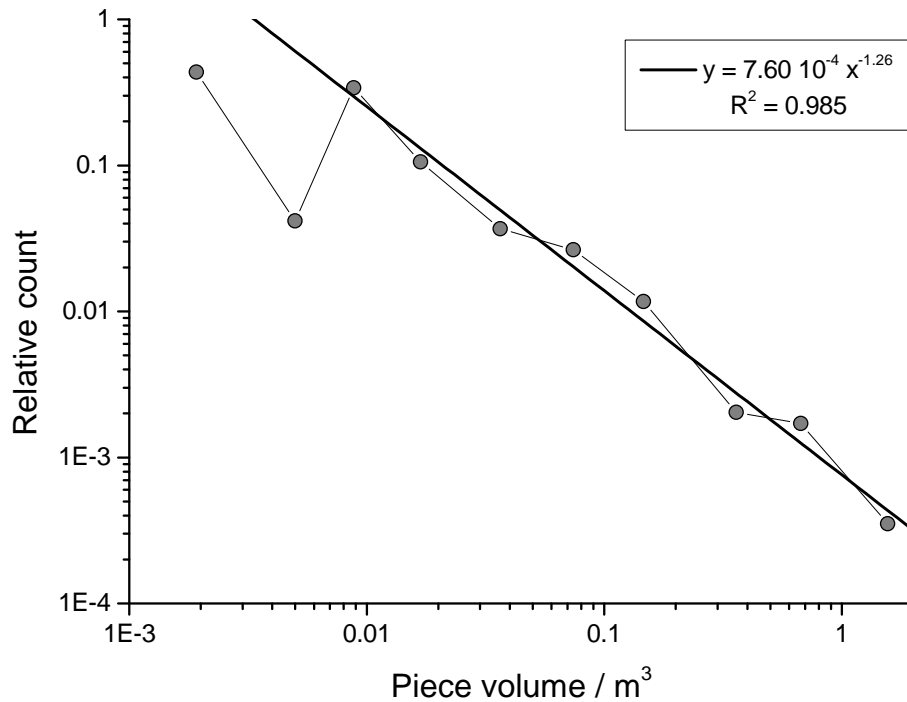


Fig. 5. Scaling distributions of piece mass for LWD locked in log jams in the Erlenbach channel.

The mass distribution of coarse particulate organic matter

J. M. Turowski et al.

Title Page	
Abstract	Introduction
Conclusions	References
Tables	Figures
◀	▶
◀	▶
Back	Close
Full Screen / Esc	
Printer-friendly Version	
Interactive Discussion	



The mass distribution of coarse particulate organic matter

J. M. Turowski et al.

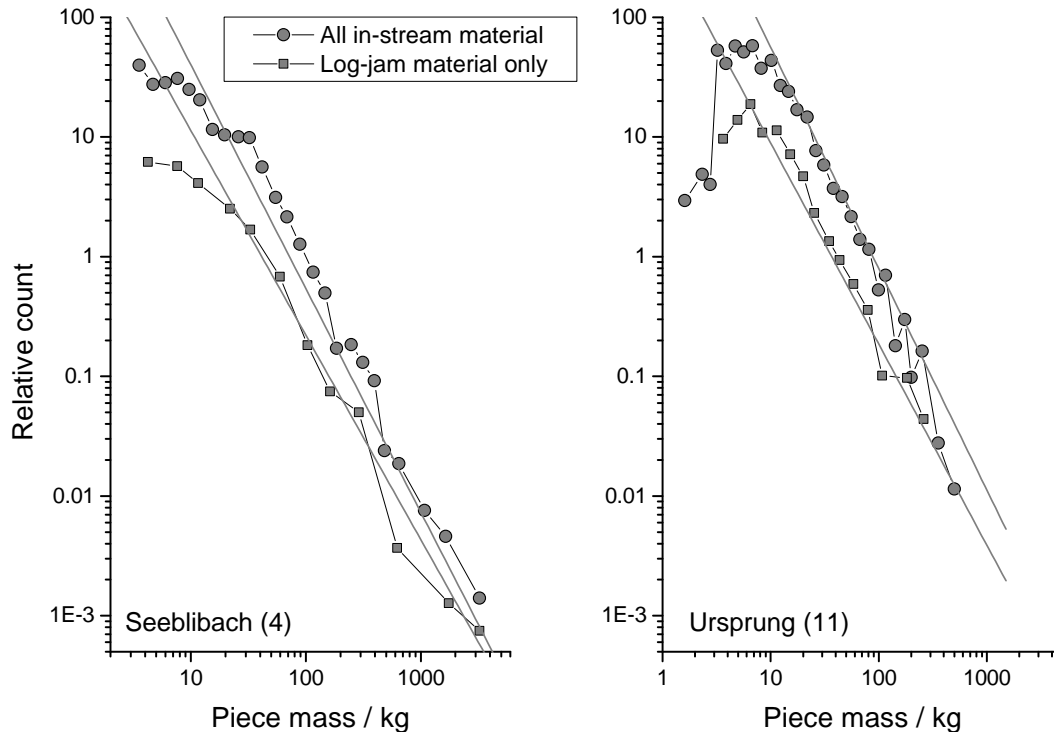


Fig. 6. Scaling distributions of piece mass for LWD in the Seeblibach (4) and Ursprung (11) (see Table 1), as examples for distributions observed in the Swiss mountain streams (Rickli and Bucher, 2006). Distributions both for material locked in log jams (square symbols) and for all material (circles) stored in the channel are shown.

Title Page

Abstract

Introduction

Conclusions

References

Tables

Figures

◀

▶

◀

▶

Back

Close

Full Screen / Esc

Printer-friendly Version

Interactive Discussion

The mass distribution of coarse particulate organic matter

J. M. Turowski et al.

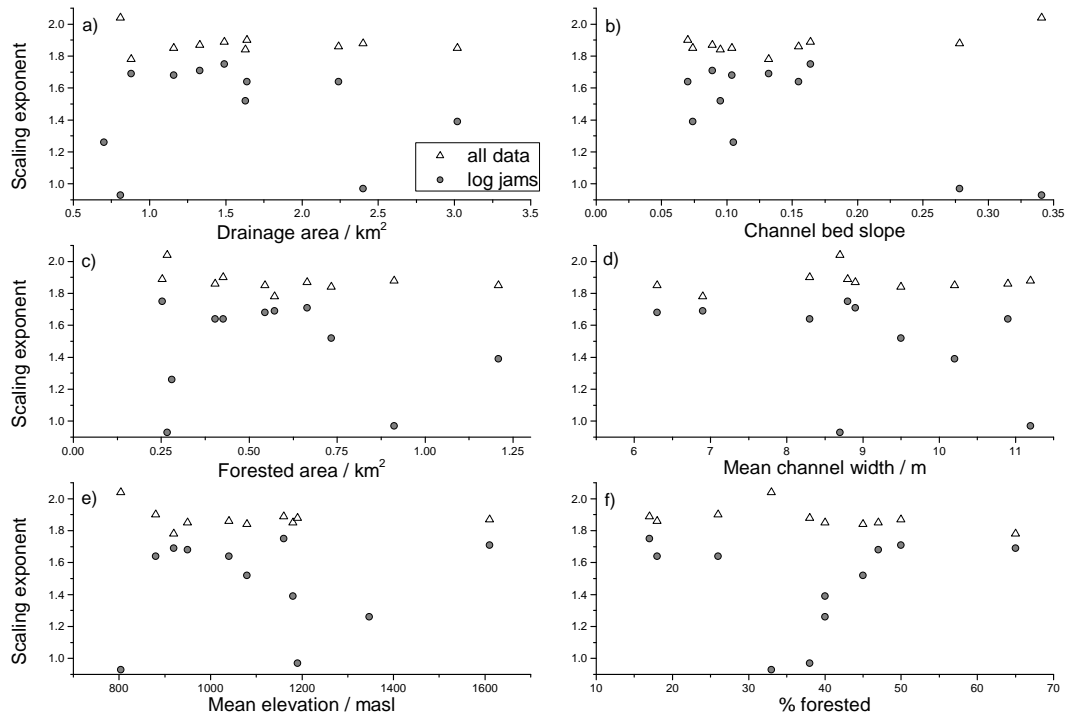


Fig. 7. Scaling exponents of eleven Swiss mountain streams (Table 1) as functions of **(a)** drainage area, **(b)** channel bed slope, **(c)** forested area, **(d)** mean channel width, **(e)** mean elevation above sea level, and **(f)** percent fraction of the catchment covered by forest. Note that the two lowest scaling exponents for log jam material at 0.93 and 0.97, corresponding to the Brüggwaldbach and Grossbach (Table 1), are based on a small number of measurement and are probably spurious. No strong correlations or trends are obvious.

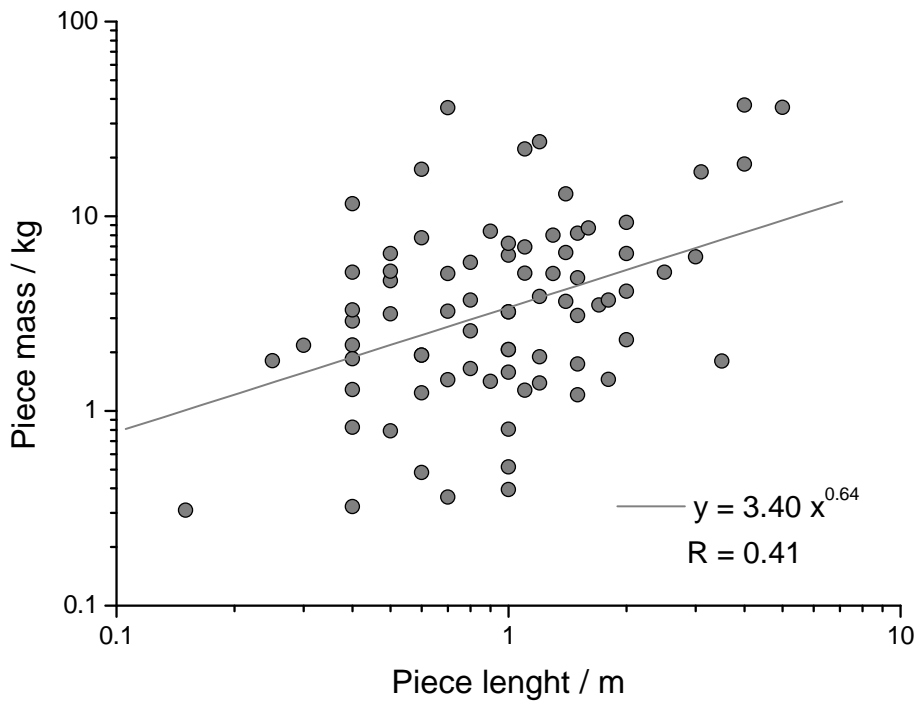


Fig. 8. Relationship between piece mass and length for material from the Erlenbach retention basin samples.

The mass distribution of coarse particulate organic matter

J. M. Turowski et al.

Title Page	
Abstract	Introduction
Conclusions	References
Tables	Figures
◀	▶
◀	▶
Back	Close
Full Screen / Esc	
Printer-friendly Version	
Interactive Discussion	



The mass distribution of coarse particulate organic matter

J. M. Turowski et al.

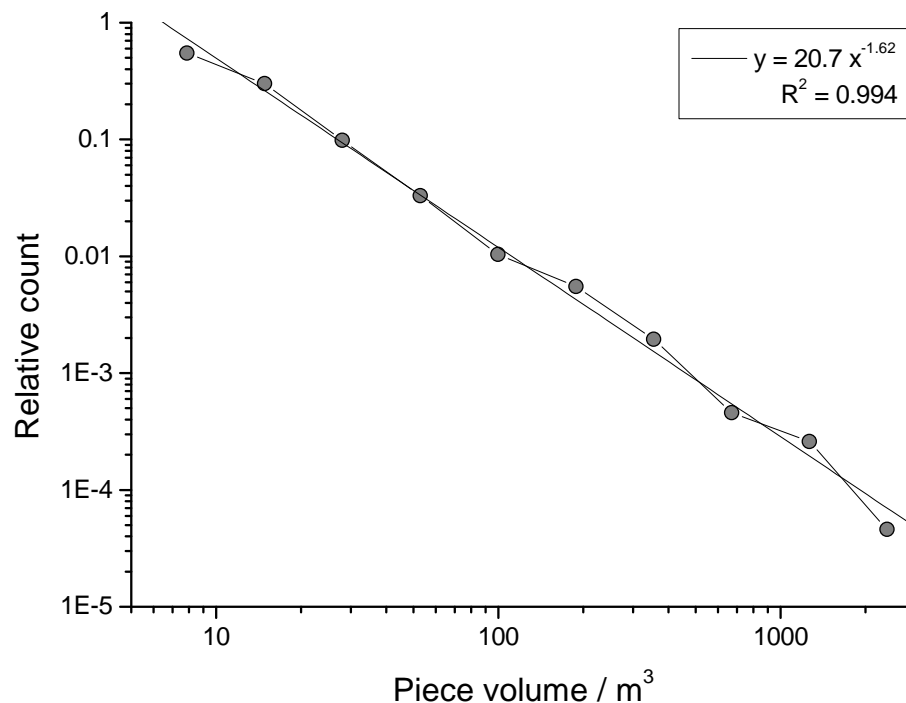


Fig. 9. Scaling distribution of piece mass for LWD transported in the Ain River, France, obtained from the data published by MacVicar and Piégay (2012) for November 2007 (the other data are similar). Piece number and mass are also related by a power law with a scaling exponent of 1.62 ($R^2 = 0.994$).